Three-Dimensional Analysis of ICRF Wave Excitation on the GAMMA 10 Central Cell

Y. YAMAGUCHI, M. ICHIMURA, A. FUKUYAMA[1], H. HOJO, S. SATO, T. MURAKAMI, Y. IMAI, T. YOKOYAMA, Y. MIYAKE, and T. IMAI
Plasma Research Center, University of Tsukuba, Tsukuba, Ibaraki 305-8577, Japan
[1]Department of Nuclear Engineering, Kyoto University, Kyoto 606-8501, Japan

(Received: 5 November 2009 / Accepted: 14 January 2010)

A three-dimensional full-wave code is newly employed to investigate the plasma production by Ion-Cyclotron Range of Frequency (ICRF) waves on GAMMA 10. The spatial structure of the excited wave fields are calculated for two types of ICRF antennas (Double Half-Turn and Nagoya Type-III) in the central cell. The plasma production by ICRF waves depends on the wave excitation in the plasma. Eigenmodes are strongly formed when the boundary conditions are satisfied. In the experiment, the saturation of the plasma density is observed when Nagoya Type-III antenna is used for the plasma production. On the other hand, remarkable increase in the plasma density has been obtained by controlling the phase difference between Double Half-Turn and Nagoya Type-III antennas. The spatial structure of the wave field is calculated, and the antenna-plasma coupling is evaluated. It is predicted that Double Half-Turn antenna strongly couples to the eigenmode, and therefore produces the higher density plasmas in the central cell.

Keywords: GAMMA 10, 3D-FEM, ICRF, Eigenmode, Double Half-Turn antenna, Nagoya Type-III antenna

1. Introduction

The radio-frequency (rf) power in the Ion-Cyclotron Range of Frequency (ICRF) is used to provide the plasma production, ion heating, and stabilization against the magneto-hydrodynamic (MHD) instability in the tandem mirror experiments [1-3]. In GAMMA 10, strong ion-cyclotron heating has achieved the high ion-temperature above 10 keV [3]. In recent years, one of the most active topics on GAMMA 10 has been a higher density plasma production in the central cell [4, 5]. In the present condition, the density is relatively low ($\sim 2\times10^{18}$ m^{-3}), which restricts the operation window for the study of the potential confinement, effective Neutral Beam Injection (NBI), and so on. To improve the tandem mirror performance, the high density plasma production is a crucial issue.

In the experiment, Nagoya Type-III (Type-III) antennas [6] and Double Half-Turn (DHT) antennas are installed at both ends of the central cell. On the standard discharge, Type-III antenna is coupled to the fast wave with the frequency of ~ 10 MHz ($\omega/\omega ci \sim 1.6$). The excited fast wave plays the role of plasma production in the central cell. DHT (6.36 MHz, $\omega/\omega ci = 1$) is used for the fundamental ion-cyclotron heating. Several methods have been adopted to produce the high density plasmas [3-5]. Recently, remarkable increase in the density was observed with a new antenna configuration, where the neighboring Type-III and DHT antennas are driven at the same frequency with controlling the phase difference ($\Delta\phi \sim 0$) between them. Achieved plasma density is ~ 5×10^{18} m^{-3}, which is more than twice as large as the conventional value.

The wave propagation may change sensitively to the density profile and the boundary conditions. In the present experimental configuration, the central cell plasma is cylindrically bounded, and the characteristic dimension is of the order of the wave length. When the boundary condition is satisfied, the wave field is strongly excited as the eigenmode. For the study of the eigenmodes, it is necessary to take into account the spatial inhomogeneity and the boundary conditions of the plasmas. In order to investigate the ICRF wave excitation, propagation, and absorption, a three-dimensional full wave code is used. The central cell is divided into the three-dimensional mesh, and the rf current straps are arranged in the shape of the DHT and Type-III antennas. The spatial structure of the wave field is calculated, and the profile of the absorbed power is evaluated. The calculations are performed for two antenna configurations, which are only Type-III and Type-III + DHT (with the phase difference of $\Delta\phi = 0$). The waves are excited with large amplitude and absorbed in the core plasma region when the DHT + Type-III antenna is used. On the other hand, the power absorption concentrates near the antenna in the case of Type-III antenna. It is suggested that the strong excitation of the waves in the core plasma region with DHT antenna is effective for high density

e-mail: yamaguti@prc.tsukuba.ac.jp

©2010 by The Japan Society of Plasma Science and Nuclear Fusion Research

plasma production.

The manuscript is organized as follows, In Sec. 2 we will describe the central cell configuration of the GAMMA 10 experiment. In Sec. 3 the experimental results is presented for high density plasma production. In Sec. 4 we will introduce the numerical calculation of the wave excitation, and compare with the experimental results.

2. GAMMA 10 Device

GAMMA 10 consists of five mirror cells, which are a central cell, two quadruple minimum-B anchor cells placed immediately outside the central cell, and the plug/barrier cells at both ends (Fig. 1). The central cell has an axisymmetric mirror configuration and is 5.6 m in length with the field strength of 0.4 T at the midplane. The mirror ratio of the central cell is 5. The anchor cell has a non-axisymmetric minimum-B field configuration and is 1.6 m in length with the field strength of 0.6 T at the midplane. Two ICRF sources (RF1 and RF2) are currently used for plasma production, heating and stabilizing against the Magneto-Hydro-Dynamic (MHD) modes. Two kinds of ICRF antennas (DHT and Type-III) are installed near both mirror throats of the central cell. Type-III antennas are driven by the RF1 system. The frequencies of RF1 (9.9 and 10.3 MHz) are selected as the fundamental ion-cyclotron resonance frequency of the hydrogen plasma near the midplane of the anchor cells. The frequency of west Type III antenna is slightly higher than the frequency of the east one in order to avoid the strong interference between two antennas. RF1 plays two roles, that is, plasma production in the central cell, and ion heating in the anchor cells for stabilizing against the MHD modes. Fast Alfvén waves excited in the central cell propagate to the anchor cell. At the flux tube with an elliptical cross section which is located between the central and the anchor cells, a part of the fast waves is converted to the slow waves and heats ions in the anchor cell [7, 8]. The production of the high beta plasma in the minimum-B anchors is necessary to sustain the plasma in the central cell [9]. DHT antennas are driven by RF2 and are used for ion heating in the central cell. The frequency of RF2 is adjusted to 6.36 MHz, which is the ion-cyclotron resonance frequency near the midplane of the central cell. A discharge is started by injecting a

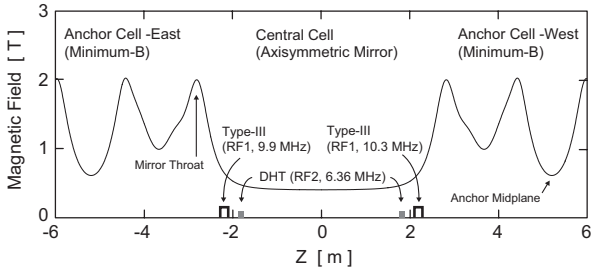

Fig. 1. Axial profile of the magnetic field strength, locations of the ICRF antennas.

short pulse (1 ms) gun-produced hydrogen plasma flows from each end, and is sustained by applying rf power in combination with hydrogen gas puffing in the central cell.

3. Experiment of high density plasma production

In the experiments, saturation in the density ($\sim 2\times10^{18}$ m^{-3}) has been observed when RF1 is used (Fig. 2) [3-5]. The cause of the density saturation is now considered as due to the eigenmode formation of the excited waves. As the optimum density exists for the waves to satisfy the boundary condition, the density will be clamped at the value on which the eigenmode is formed. For effective excitation of the eigenmodes, a new antenna configuration was introduced. The previous theoretical work suggests that DHT antenna is more effective for the fast wave excitation [5]. Shown in Fig. 3, DHT antenna is driven by the frequency of neighboring

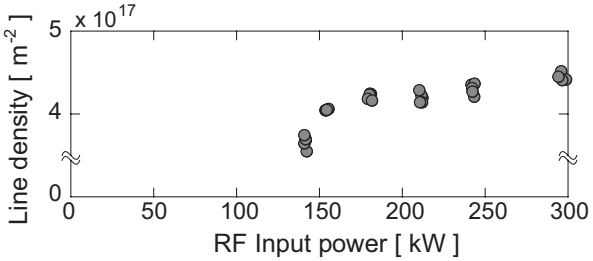

Fig. 2. RF input power dependence of the line density. Saturation of the density has been observed with RF1. The line-density of 4×10^{17} m^{-2} corresponds to the density of 2×10^{18} m^{-3} at the core

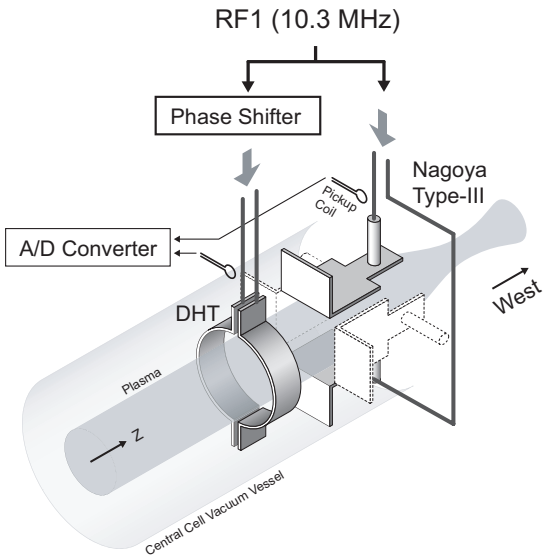

Fig. 3. Experimental arrangement for controlling the phase difference between west DHT and west Type-III antenna in the central cell. The phase difference is monitored by use of pickup coil located close to the antennas.

Type-III antenna. RF1 signal (10.3 MHz) is split in two, and a part is newly connected to the amplifier of DHT antenna via a phase shifter. The experiment was performed to control the phase difference between two antennas. The input power is evaluated by use of the bi-directional coupler installed outlet of the rf power amplifier. The loss due to a mismatch of the impedance is taken into account to derive the input power. In order to measure the antenna phase, rf current on the antennas is detected with pickup coils, which are installed close to the antenna. In Figure 4, temporal evolution of the line-integrated density is shown.

In the experiments, the phase difference was changed for each discharge. Whole power input for plasma production was fixed to about 240 kW. In Figure 5, the electron density at the plasma core is plotted versus the phase difference. The core plasma density is estimated by the interferometer, which has the multiple measurement channels in the radial direction. As is clearly indicated in the figure, an optimum phase difference exists for the plasma production in the present density range. Sometimes plasmas can not be sustained when the phase differences largely away from the optimum one. Figure 6 gives the rf power dependence of the plasma density. The phase difference between two antennas was set to the optimum one. The density considerably increases with applied rf power. Together with the rf power, gas fuelling rate is also increased. In this experiment, the density is enhanced up to ~5×10^{18} m^{-3} (corresponding line density is ~8×10^{13} cm^{-2}), which is more than twice as large as the conventional value. No saturation in the density has been observed. And more increase in the density can be expected with increasing the rf power.

4. Three-Dimensional Analysis of the Wave Excitation

While the phase controlled antennas have complicated rf current path around the inhomogeneous plasma, it is important to carry out detailed wave analysis in the precise central cell geometry. In this work, the effect of the antenna structure to the wave excitation is computationally evaluated by use of a three-dimensional full wave code (PAF/WF3: Plasma Analysis by FEM / Wave analysis by FEM 3D). This code is developed by one of the authors; Prof. A. Fukuyama in Kyoto University. This code solves the Maxwell's equation for the wave electric-field as a boundary-value problem using the finite element method (FEM). In the model, it is assumed that the cold and inhomogeneous plasma surrounded by the conducting walls. The power absorption with the collisional damping is described by introducing effective collisions in the dielectric tensor. Figure 7 shows the generated finite

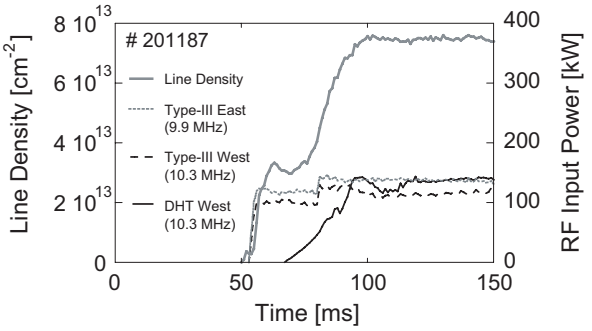

Fig. 4 The temporal evolution of the line-integrated density on typical discharge is shown together with the applied rf power for each antenna.

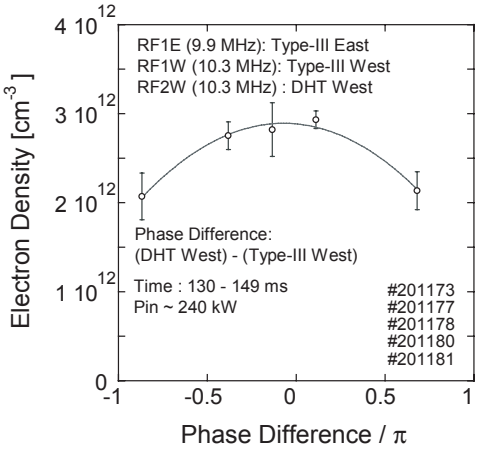

Fig. 5. Antenna phase dependence of the density at the core region is shown. The phase-shift of DHT from Type-III is measured. The amount of power input was fixed to about 240 kW. The density profile was estimated from 130 to 149 ms at 5ms intervals. It is clearly seen that an optimum phase difference exists for the plasma production.

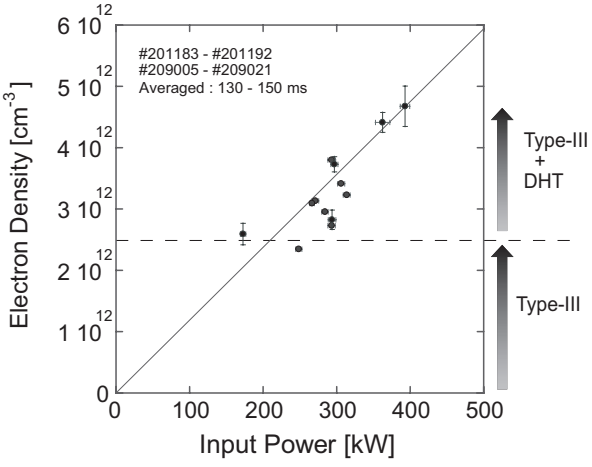

Fig. 6. RF power dependence of the plasma density. The phase difference between two antennas was fixed to the optimum one.

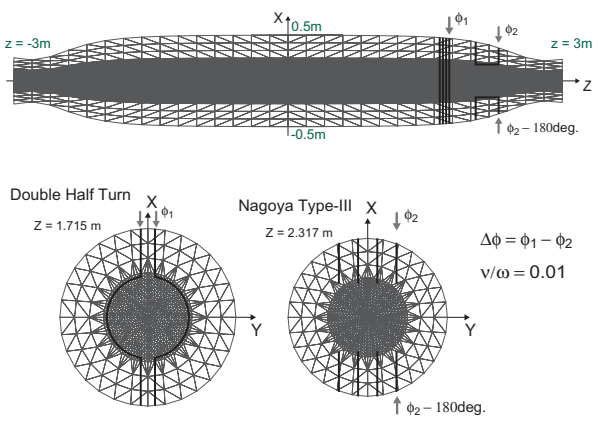

Fig. 7. Finite element mesh of the central cell. Configuration of DHT and Type-III antennas are shown.

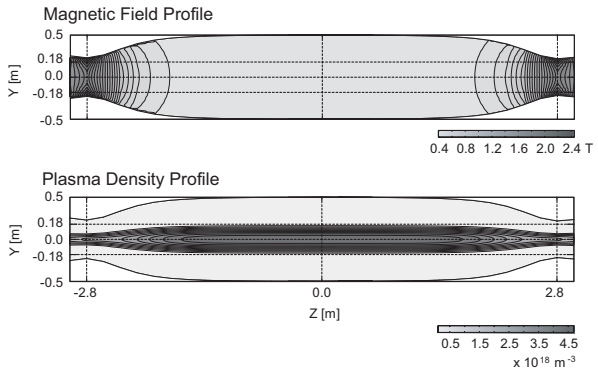

Fig. 8. The parameters used in the calculations. Contour plots of the external magnetic field and the plasma density on y-z space.

element mesh. The element size is optimized in order to have sufficiently large numbers of spatial elements within the core plasma region. The number of finite elements within the system was 117270 in this calculation. DHT and Type-III antennas are approximated by external rf current straps. To take into account the width of the antennas, each antenna is composed of four current straps. In the present calculations, rf current on each strap is assumed to be same. The external magnetic field and the plasma density can be non uniform in all directions. Here we used the magnetic field of the central cell and the measured profile of the density (Fig.8).

In order to identify the mode of the excited wave, spatial structure of the electric-field is calculated. The peak density is set to 5×10^{18} m^{-3}. The rf power radiated from the antenna is fixed to be 100 kW. For the case of DHT + Type-III antennas, the phase difference between two antennas is set to $\Delta\phi = 0$. Figure 9 shows the electric-field vector on each node of the finite-element mesh on the x-y plane at the mid-plane (z = 0). And the contour plot of the radial electric-field is given in same figure. By changing

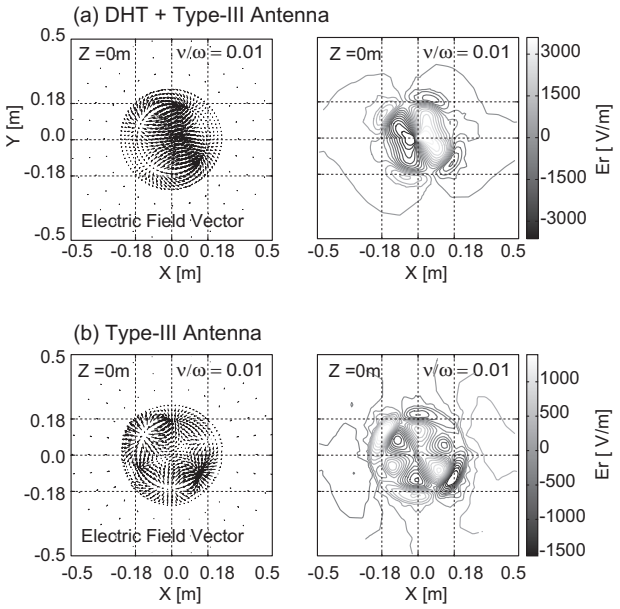

Fig. 9. The electric-field vector on each node, and the profile of the radial component of the wave electric field. It is clearly shown that DHT + Type-III (the phase difference between two antennas is $\Delta\phi = 0$) excites m = +1 mode. In the case of Type-III antenna, m = +3 mode is dominantly excited at the core plasma region.

the phase of the rf current from 0 to 360 degrees with keeping the phase difference between DHT and Type-III to be $\Delta\phi = 0$, we remarked the time-variation of the field profiles. Then, it is found that the electric-field vector rotates right-handed (co-rotation with electron cyclotron motion) at the core plasma region (r < 0.18m), and rotates left handed at the peripheral plasma region. In addition, we confirmed that the global structure of the electric fields rotates right-handed, which means the sign of the azimuthal mode number is positive [10]. The excited waves are suggested to be the fast wave. It is clearly seen that the antenna strongly couples to m = +1 mode at the core plasma region in case of DHT + Type-III (Fig. 9(a)). On the other hand, the radial electric field excited by Type-III antenna indicates the appearance of the m = +3 mode (Fig. 9(b)). The amplitude of the excited electric-field at the core plasma region is small as compared with the case of DHT + Type-III antenna. Figure 10 gives the contour plots of radial electric-field and absorbed power on the y-z plane for two cases. For the case of DHT + Type-III antenna, which is shown in Fig 10(a), it seems that the antenna strongly couples to the axial eigenmode and the power is dumped on the core plasma region. In the case of Type-III (Fig.10(b)), however, the amplitude of the coupled wave is small in the core plasma, and the power absorption concentrates around the antenna. From the calculation results, it is suggested that the strong excitation of the waves in the core plasma region is effective for high density plasma production.

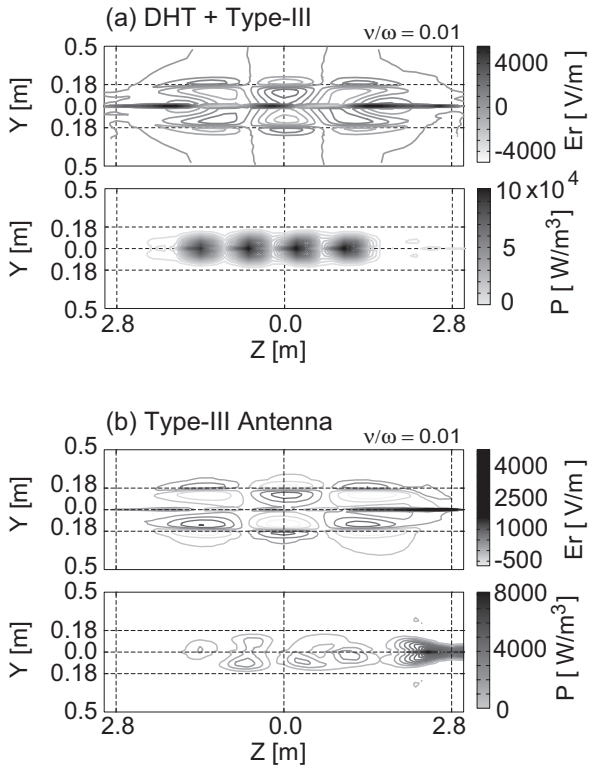

Fig. 10. The contour plot of the radial electric field and absorbed power on y-z plane for the cases of the Type-III antenna and DHT + Type-III antenna (the phase difference between two antennas is $\Delta\phi = 0$).

The antenna-plasma coupling is computationally evaluated to compare with the experimental result of the antenna phase control between DHT and Type-III antennas. The calculation is performed by changing the phase difference (0 ~ 360deg.) and the plasma density (0.2×10^{18} ~ 10×10^{18} m^{-3}). Figure 11 shows the loading resistance of each antenna as the functions of the phase difference and the plasma density. From the viewpoint of the antenna-phase dependence, the loading resistances of two antennas have different characteristics. As is clearly seen in Fig. 11(a), the loading resistance of Type-III antenna depends strongly on the phase difference. The optimum phase difference is shown to be $\Delta\phi \sim -74$ deg., which is near the experimental observation. On the other hand, the loading resistance of DHT antenna has less dependence on the phase difference as compared with Type-III antenna. As for the density dependence, several sharp peaks of the loading resistance can be seen on each figure. When the density is changed and the eigenmode is strongly excited, the loading resistance indicates the peak value. In comparison to Type-III antenna, the loading peaks of DHT antenna have much higher values. This result indicates that DHT antenna couples to the eigenmodes stronger than Type-III antenna. Therefore, in the phase controlled experiment with DHT + Type-III antenna, it is suggested that DHT antenna takes main role

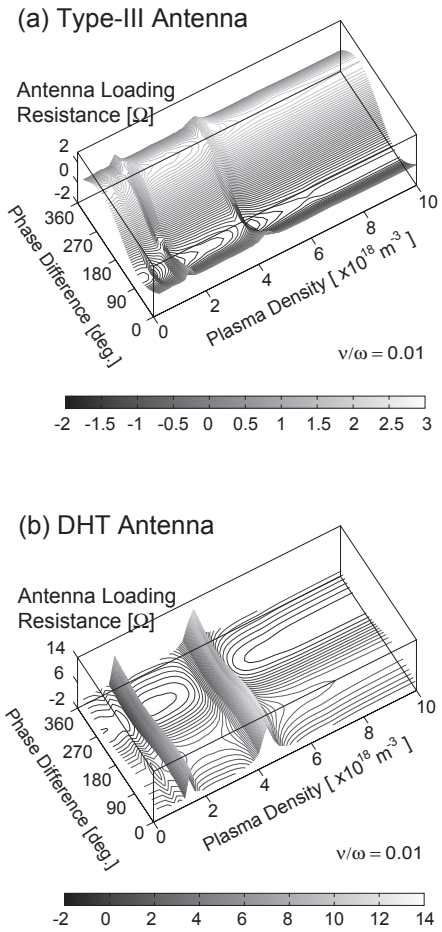

Fig. 11. The antenna loading resistance as the function of the phase difference and the plasma density.

for the density increase.

In the calculation of Fig. 11, we reduced the number of finite elements from 117270 to 18000 because of the limitation of the calculation time. Due to rather coarse FEM grid, the field structure which has the small wave length cannot be described. If the calculation is performed with the large element-number of 117270, detailed structure of the excited waves can be described as shown in Fig. 10(a). In Figure 10(a), the excited wave has the averaged wave length of ~2.4m on Z axis at the core plasma density of 5×10^{18} m^{-3}. However, in case of Fig. 11, the excited wave has the averaged wave length of ~5.6m on Z axis around the loading peak at ~4.4×10^{18} m^{-3}. This difference is caused by the reduction of spatial resolution of the finite element mesh. If the number of finite elements is large enough, the eigenmodes which have the small wave length will appear. As the result, the number of the loading peaks may increase in the density range on Fig.11.

5. Summary

We have presented the first application of the

three-dimensional wave calculation code to the GAMMA 10 experiment. The remarkable increase in the plasma density is experimentally observed by use of new antenna configuration, where the phase difference is controlled between neighboring DHT and Type-III antennas. The spatial structure of the wave field is calculated, and the degree of antenna-plasma coupling is evaluated. It is predicted that DHT antenna is effective to produce the higher density plasmas in the central cell.

Acknowledgment

The authors acknowledge the support of GAMMA 10 group. This work is partly supported by the bi-directional collaborative research program of National Institute for Fusion Science, Japan (NIFS09KUGM042).

References

[1] S. N. Golovato et al., Physics of Fluids **31**, 3744 (1988)
[2] J. R. Ferron et al., Physical Review Letters **51**, 1955 (1983)
[3] M. Ichimura et al., Physics of Plasmas **8**, 2066 (2001)
[4] Y.Yamaguchi et al., Plasma Physics and Controlled Fusion, **48**, 1155 (2006).
[5] Y.Yamaguchi et al., Fusion Science and Technology, **55**,No. 2T, 106 (2009).
[6] T. Watari et al., Nuclear Fusion **22**, 1359 (1982)
[7] M. Inutake, et al., Physical Review Letters **31**, 3397 (1990)
[8] H. Hojo, et al., Physical Review Letters **66**, 1866 (1991)
[9] M. Ichimura et al., Nuclear Fusion **28**, 799 (1988)
[10] T. Kaneko et al., Plasma Fusion Res. **2**, 038 (2007)